TABLE A2. DETERMINED VALUES OF $E_{z,ml}$ USED IN THE CALCULATION OF E_o

1-Zone/Tray $E_{z,ml}$ (= $E_{z,mg}$)	3-Zones/Tray $E_{z,ml}$	12-Zones/Tray $E_{z,ml}$
0.5	0.250	0.0775
0.6	0.333	0.1139
0.7	0.445	0.1707
0.8	0.570	0.254
0.9	0.760	0.437
1.0	1.0	1.0

since for the liquid flow the mixing zones are arranged in series. For this reason the value of the mixing zone efficiency has to be determined in such a way that for no vapor entrainment the overall column efficiency E_o for every case corresponds with the E_o's calculated on the basis of $E_{z,mv}$. In this way Figure A2 also applies for the calculations based on $E_{z,ml}$. The values of $E_{z,ml}$ are given in Table A2.

The values of $E_{z,ml}$ given in Table A2 are used to calculate the effect of vapor entrainment on the overall column efficiency. The results for three mixing zones per tray and for plug-flow are given in Figure 7.

Intraparticle-Forced Convection Effect in Catalyst Diffusivity Measurements and Reactor Design

Intraparticle forced convection was considered in order to explain experimentally observed changes in effective diffusivity (apparent) with flowrate, when measures are carried out in fixed beds.

A complete model taking into account intraparticle diffusion and forced convection together with film diffusion is derived in order to analyze diffusivity measurements by physical methods, both in perfectly mixed reactors and fixed beds.

The experiments were carried out with hydrogen tracer in a partial oxydation catalyst.

Implications of the use of such "apparent" effective diffusivities in reactor design are discussed, showing that errors of 100% can be made.

A. E. RODRIGUES
Department of Chemical Engineering
University of Porto
Porto Codex, Portugal

BUM J. AHN
and
ANDRÉ ZOULALIAN
Département de Génie Chimique
Université de Technologie de Compiègne
Compiègne, France

SCOPE

Experimental data on effective diffusivities, measured by unsteady state techniques show that increasing the flowrate, greater values for the effective diffusivity (apparent) are obtained (Boersma-Klein and Moulijn,, 1979; Ahn, 1980). These findings have been sometimes explained by measurements inaccuracies, but this explanation can hardly be acceptable when changes on apparent effective diffusivities are of one order of magnitude for the same changes in flowrate.

On the other hand Nir and Pismen (1977) analyzed the influence of intraparticle-forced convection on effectiveness factors, showing that this mechanism can be important for large pore catalysts, specially with liquid phase reactions.

In the present work, we tried to explain the results obtained in a series of experiments carried out over a range of flowrates corresponding to changes of one order of magnitude in Reynolds number (Re = 10 to 100) for hydrogen, as a tracer, in a highly porous catalyst for the partial oxydation of butene to maleic anhydride (Rhone Poulenc BM 329). The questions to be answered are: Can intraparticle forced convection explain the variation of the measured effective diffusivity with flowrate? If so, how do we predict the intraparticle convection velocity for given operating conditions?

Finally the aim of this work was to check if, for practical purposes, significant implications result when apparent effective diffusivities are used in reactor design.

CONCLUSIONS AND SIGNIFICANCE

A series of experiments for the measurement of effective diffusivity was carried out in a fixed bed of small tube diameter/particle diameter ratio—single pellet string reactor of Scott et al. (1974)—using hydrogen as nonadsorbable tracer and a Rhone Poulenc BM 329 catalyst (catalyst used for partial oxydation of butene to maleic anhydride based on vanadium and phosphorus oxydes) at 293 K.

Sharp variations of the measured effective diffusivity with flowrate were observed, the values being obtained from optimization based on a transfer function of the system which takes into account only one mechanism inside the particle (intraparticle diffusion).

We investigated if intraparticle-forced convection could explain these findings. We first developed the model equations and the transfer functions of the current systems for physical measurements of effective diffusivity.

We were able to show that the measured (apparent) effective diffusivity, $\tilde{D}_{\text{eff}}$, is related to the true (constant) effective dif-

---

Correspondence concerning this paper should be addressed to A. E. Rodrigues.
0001-1541-82-5941-0541-$2.00.

fusivity, D_{eff}, and to the intraparticle Peclet number, $\lambda = v_o l/D_{\text{eff}}$ (v_o, intraparticle flow velocity; l, characteristic dimension of the particle) by $\tilde{D}_{\text{eff}} = D_{\text{eff}}/f(\lambda)$, where $f(\lambda) = 3/\lambda\,(1/th\lambda - 1/\lambda)$.

Furthermore, we were able to predict the intraparticle convective flow, by linking the pressure drops across the reactor and across the particle, provided one can estimate the particle permeability.

Finally, implications on reactor design have been quantified showing that the use of "apparent" effective diffusivities could lead to errors of 100% in effectiveness factor calculations, and so in reactor size.

Effective diffusivity in catalysts is an important parameter for reactor design; its measurement is usually done by steady state diffusion techniques, such as the Wicke-Kallenbach method (1941) or by unsteady state methods.

The first class gives only information on macropore diffusion (Kawazoe and Takeuchi, 1974); no indication on solid anisotropy and dead-end pores is obtained and since temperature and pressure are limited, measurements at reaction conditions cannot easily be made (Youngquist, 1970). In any case the method can be used for catalysts in which $D_{\text{eff}} > 10^{-3}$ cm^2/s.

Unsteady state methods can be used either with perfectly mixed reactors or fixed beds, applying the principles of chromatography theory (Cerro and Smith, 1970; Choudary, 1974; Furusawa et al., 1976). A special and interesting method is that of Scott et al. (1974) who used the single pellet string reactor (SPSR), i.e., a tube with a small ratio between tube diameter and particle diameter, d_t/d_p.

A look at the published literature shows that some experimental observations have not been fully explained. Among them one can mention the sharp decrease of D_{eff} with macroporosity (Dogu and Smith, 1976); however, as pointed out by Smiljanic (1977) the effective diffusivity is not a single monotonic function of porosity.

The most interesting aspect, from our point of view, is the dependency of the measured effective diffusivity on flowrate reported by several authors. Dogu and Smith (1976) reported that the accuracy of diffusivity measurements is 50–100% or more, from the values, they present variations of $\tilde{D}_{\text{eff}}$ with flowrate being observed. Boersma-Klein and Moulijn (1979) used SPSR-obtained values for the effective diffusivity of helium in silica at 293 K which change from 1.5×10^{-3} cm^2/s to 2.2×10^{-3} cm^2/s when the Reynolds number goes from 36.4 to 66.6.

These "discrepancies" are not due to film mass transfer intrusions as pointed out by the authors, who preferred to explain the results on the basis of inaccurate measurements. Also, they recommend that one should use the intermediate velocities for diffusivity determination experiments since the accuracy is reasonable in that range.

Recently, Ahn (1980) using the SPSR technique, developed by Scott et al. (1974), made similar experimental observations on the variation of the measured effective diffusivity with flowrate. The system used was hydrogen/vanadium-phosphorus oxydes catalyst. Sharp variations of $\tilde{D}_{\text{eff}}$ were reported by changing the Reynolds number over an order of magnitude (Re = 10 to 100).

These observations were the starting point for this work. The aim of the paper is to explain these trends on the basis of the effect of intraparticle forced convection and also look at the implications on reactor design when a measured $\tilde{D}_{\text{eff}}$ (at a given flowrate) is used in Thiele modulus calculations (Rodrigues, 1980a).

ANALYSIS OF DIFFUSIVITY MEASUREMENTS IN PERFECTLY MIXED REACTORS AND FIXED BEDS

Physical methods for diffusivity measurements have been carried out both in the perfectly mixed reactor of Berty type (Berty, 1974) and fixed beds (SPSR).

In the following, the model equations for each situation are briefly derived leading to the transfer function of the systems, from which the moments of the impulse response are calculated and finally the effective diffusivity determined.

Perfectly Mixed Reactor

For a nonadsorbable tracer and isothermal operation, the model equations are the unsteady state mass balances for the entire system and for the catalyst particle (slab geometry), respectively

$$Qc_o = Qc + v_f \frac{dc}{dt} + \beta v_s \frac{d\langle c'\rangle}{dt} \tag{1}$$

and

$$D_{\text{eff}} \frac{\partial^2 c'}{\partial x^2} - v_o \frac{\partial c'}{\partial x} = \frac{\partial c'}{\partial t} \tag{2}$$

where $c_o, c, \langle c'\rangle$ are the fluid-phase concentration at the inlet, outlet and the average concentration inside the particle, respectively; Q is the flowrate; v_f and v_s, the fluid volume outside the particles and the solid volume, respectively; β, the intraparticle porosity; x and t, the space particle coordinate and time, respectively; D_{eff}, the true effective diffusivity; and v_o, the intraparticle flow velocity (convection term).

The boundary conditions are, for the particle

$$x = 0, \qquad c' = c_s' \tag{3a}$$

$$x = 2l, \qquad c' = c_s' \tag{3b}$$

and for the reactor

$$t = 0, \qquad c = c' = 0 \tag{3c}$$

where l is the half thickness of the catalyst.

Introducing reduced quantities $\rho = x/l$, $\epsilon = v_f/V$ (ϵ, porosity; V, total volume of the reactor) and the characteristic times

$\tau = V/Q$ space time

$\tau_D = l^2/D_{\text{eff}}$ internal diffusion time

$\tau_C = l/v_o$ intraparticle convection time

one gets for the particle mass balance

$$\frac{1}{\tau_D}\frac{\partial^2 c'}{\partial \rho^2} - \frac{1}{\tau_C}\frac{\partial c'}{\partial \rho} = \frac{\partial c'}{\partial t} \tag{4}$$

The characteristic roots are

$$r_1, r_2 = \frac{\tau_D}{2\tau_C} \pm \sqrt{\frac{\tau_D^2}{4\tau_C^2} + \tau_D s} \tag{5}$$

and the transfer function between the particle surface concentration and the concentration in any point inside the catalyst is

$$\frac{\overline{c'}(s)}{\bar{c}_S'(s)} = \frac{(e^{2r_2}-1)e^{r_1\rho} - (e^{2r_1}-1)e^{r_2\rho}}{e^{2r_2} - e^{2r_1}} \tag{6}$$

where $\overline{c'}(\rho,s)$ denotes the Laplace transform of $c'(\rho,t)$ with respect to time t. The mean particle concentration in the Laplace domain is

$$\langle \bar{c}'\rangle = \bar{c}_S' \frac{(e^{2r_2}-1)(e^{2r_1}-1)}{e^{2r_2}-e^{2r_1}} \frac{\sqrt{(\tau_D^2/4\tau_C^2) + \tau_D s}}{\tau_D s} \tag{7}$$

and since $\langle \bar{c}'\rangle = \overline{\langle c'\rangle}$ and $\bar{c}'_S = \bar{c}$ we can replace this quantity in the transform of Eq. 1 leading to the transfer function of the perfectly mixed reactor

$$G(s) = \bar{c}/\bar{c}_o = \left\{1 + \epsilon\tau s + (1-\epsilon)\beta \frac{\tau}{\tau_D}\sqrt{\frac{\tau_D^2}{4\tau_C^2} + \tau_D s}\; \frac{(e^{2r_2}-1)(e^{2r_1}-1)}{e^{2r_2}-e^{2r_1}}\right\}^{-1} \tag{8}$$

The moments of the impulse response are then obtained by the relationship $\mu_n = (-1)^n \partial^n G(s)/\partial s^n |_{s=0}$; finally

$$\mu_1 = \epsilon\tau + (1-\epsilon)\beta\tau = \gamma\tau \tag{9a}$$

$$\mu_2 = 2\mu_1^2 + 2(1-\epsilon)\beta\tau\tau_C \left(\frac{1}{th\lambda} - \frac{1}{\lambda}\right) \tag{9b}$$

Introducing $\lambda = \tau_D/\tau_C$, which simply is an intraparticle Peclet number comparing intraparticle convective and diffusive flows, the variance of the impulse response is expressed by

$$\sigma^2 = \mu^2 - \mu_1^2 = \gamma^2\tau^2 + \frac{2}{3}(1-\epsilon)\beta\tau\tau_D f(\lambda) \tag{10}$$

where

$$f(\lambda) = \frac{3}{\lambda}\left\{\frac{1}{th\lambda} - \frac{1}{\lambda}\right\}$$

when λ goes from 0 to ∞, $f(\lambda)$ changes between 1 and 0.

The limiting situation corresponding to the absence of intraparticle forced convection is easily handled; in fact for $\tau_C = \infty$ or $\lambda = 0$, Eqs. 6 and 7 become respectively

$$\frac{\bar{c}'}{\bar{c}'_S} = \frac{ch\, r(1-\rho)}{ch\, r} \tag{6a}$$

and

$$\langle \bar{c}' \rangle = \bar{c}'_S \frac{th\, r}{r} \tag{7a}$$

where $r = \sqrt{\tau_D s}$. Similarly Eq. 8 will be now

$$G(s) = \left\{1 + \epsilon\tau s + (1-\epsilon)\beta\frac{\tau}{\tau_D}\sqrt{\tau_D s}\, th\sqrt{\tau_D s}\right\}^{-1} \tag{8a}$$

If only internal diffusion is taken into account in the analysis of the impulse response, the variance is calculated by

$$\tilde{\sigma}^2 = \gamma^2\tau^2 + \frac{2}{3}(1-\epsilon)\beta\tau\tilde{\tau}_D \tag{10a}$$

The authors who neglected the convection effect measured in fact a diffusion time, $\tilde{\tau}_D$ which is related with the true diffusion time, τ_D by comparing Eqs. 10 and 10a, i.e.

$$\tilde{\tau}_D = \tau_D f(\lambda) \tag{11}$$

If the film mass transfer resistance is considered one should add to Eqs. 1 to 3 the kinetic law

$$k_f a(c - c_S) = \beta\frac{d\langle c' \rangle}{dt} \tag{12}$$

where a is the specific area of the particle ($a = 1/l$ for slab geometry) and k_f is the film mass transfer coefficient. In this case

$$G_1(s) = \left\{1 + \epsilon\tau s + \frac{\beta(1-\epsilon)\tau}{\tau_D}\frac{M(s)}{1 + \dfrac{M(s)}{\mathrm{Bi}_m}}\right\}^{-1} \tag{13}$$

where $\mathrm{Bi}_m = \tau_D/\tau_f$ is the Biot mass number, $\tau_f = \beta l/k_f$ is the external diffusion time, and

$$M(s) = \sqrt{\frac{\tau_D^2}{4\tau_C^2} + \tau_D s}\,\frac{(e^{2r_2}-1)(e^{2r_1}-1)}{e^{2r_2} - e^{2r_1}}$$

The moments of the impulse response will be then

$$\mu_1 = \gamma\tau \tag{14a}$$

$$\mu_2 = 2\gamma^2\tau^2 + \frac{2}{3}\beta(1-\epsilon)\tau\tau_D\left\{f(\lambda) + \frac{3}{Bi_m}\right\} \tag{14b}$$

$$\sigma^2 = \gamma^2\tau^2 + \frac{2}{3}\beta(1-\epsilon)\tau\tau_D\left\{f(\lambda) + \frac{3}{\mathrm{Bi}_m}\right\} \tag{14c}$$

Fixed Beds

Assuming an infinite fixed bed reactor where axial dispersion, film diffusion, intraparticle forced convection and diffusion are considered, the system equations are Eqs. 2 and 12 coupled with the mass balance over a volume element of the bed, i.e.

$$\epsilon D_{ax}\frac{\partial^2 c}{\partial z^2} = u_0\frac{\partial c}{\partial z} + \epsilon\frac{\partial c}{\partial t} + (1-\epsilon)\beta\frac{\partial\langle c' \rangle}{\partial t} \tag{15}$$

where D_{ax} is the axial dispersion coefficient; u_o, the superficial velocity; z, the axial coordinate in the bed; and c is now a function of z and t.

Introducing $z^* = z/L$ (L, length of the bed), $\tau = L/u_o$ and Pe $= u_o L/\epsilon D_{ax}$ (Peclet number), transforming Eq. 15 relatively to time and taking into account that $\bar{c}'_S = \bar{c}_S$ we get from Eqs. 7 and 12

$$\langle \bar{c}' \rangle = \bar{c}_S\frac{M(s)}{\tau_D s}$$

$$\bar{c}_S = \bar{c}\frac{1}{1 + \dfrac{M(s)}{Bi_m}}$$

and finally

$$\frac{1}{\mathrm{Pe}}\frac{d^2\bar{c}}{dz^{*2}} - \frac{d\bar{c}}{dz^*}$$

$$-\left\{\epsilon\tau s + (1-\epsilon)\beta\frac{\tau}{\tau_D}\frac{M(s)}{1 + \dfrac{M(s)}{\mathrm{Bi}_m}}\right\}\bar{c} = 0 \tag{16}$$

The characteristic roots are now

$$r_1, r_2 = \frac{\mathrm{Pe}}{2}\left\{1 \pm \sqrt{1 + \frac{4N(s)}{\mathrm{Pe}}}\right\} \tag{17}$$

where $N(s)$ is the term in brackets in Eq. 16.

The transfer function of the fixed bed is then

$$G(s) = \frac{\bar{c}}{\bar{c}_o} = \exp\left\{\frac{\mathrm{Pe}}{2}\left(1 - \sqrt{1 + \frac{4N(s)}{\mathrm{Pe}}}\right)\right\} \tag{18}$$

The moments of the impulse response are

$$\mu_1 = \gamma\tau \tag{19a}$$

$$\mu_2 = \gamma^2\tau^2\left(1 + \frac{2}{\mathrm{Pe}}\right) + \frac{2}{3}(1-\epsilon)\beta\tau\tau_D\left\{f(\lambda) + \frac{3}{\mathrm{Bi}_m}\right\} \tag{19b}$$

Limiting cases can be easily obtained for:

$\lambda = 0$, absence of intraparticle forced convection
Pe $= \infty$, plug flow of the fluid phase
$\mathrm{Bi}_m = \infty$, film mass transfer resistance negligible

Again, the equivalence between this complete model and that considered previously by Ahn (1980), in which forced convection inside particles is not taken into account leads to Eq. (11), i.e., $\tilde{\tau}_D = \tau_D f(\lambda)$.

On this basis, it is easily seen that with the simplified model we obtain from a chromatographic peak a value $\tilde{\tau}_D$ (at a given flowrate), which is always smaller than τ_D (the true diffusion time); then, it becomes

$$\tilde{D}_{\mathrm{eff}} = D_{\mathrm{eff}}/f(\lambda) \tag{20}$$

or $\tilde{D}_{\mathrm{eff}} > D_{\mathrm{eff}}$. At this moment one can understand why $\tilde{D}_{\mathrm{eff}}$ increases with the flowrate; in fact increasing the flowrate leads to an increase in the intraparticle Peclet number, λ and then $\tilde{\tau}_D$ decreases.

ANALYSIS OF EXPERIMENTAL RESULTS

Diffusivity measurements were carried out in both systems mentioned above. Changes in flowrate were only made in fixed bed measurements; so, the characteristics of the reactor and catalyst used in the experiments are reported in Table 1.

The catalyst is based on vanadium and phosphorus oxydes stabilized by copper; the crystalline structure has groups (VO_6)

TABLE 1. REACTOR AND CATALYST CHARACTERS CHARACTERISTICS

Reactor (Ahn, 1980)
Length of the test section, $L = 30$ cm
Tube diameter, $d_t = 2.12$ cm
Tracer:Hydrogen
Carrier gas:Air
Temperature, $T = 293$ K
Porosity, $\epsilon = 0.676$

*Catalyst for Partial Oxydation of Butene to Maleic Anhydride**
Vanadium and Phosphorus Oxydes Stabilized by Copper
Particle Diameter, $d_p = 0.45$ cm
Absolute Density, $\rho_v = 2.84$ g/cm^3
Apparent Density, $\rho_a = 1.31$ g/cm^3
Specific Area, S(B.E.T.) = 4.3 m^2/g
Porous Volume, $V_p = 0.41$ cm^3/g
Intraparticle Porosity, $\beta = 0.537$
Mean Pore Diameter, $\bar{d} = 10^4$ Å (No Pores Smaller Than 200 Å)

* Rhone-Poulenc catalyst BM 329 (*Tech.Bull.*, 1980).

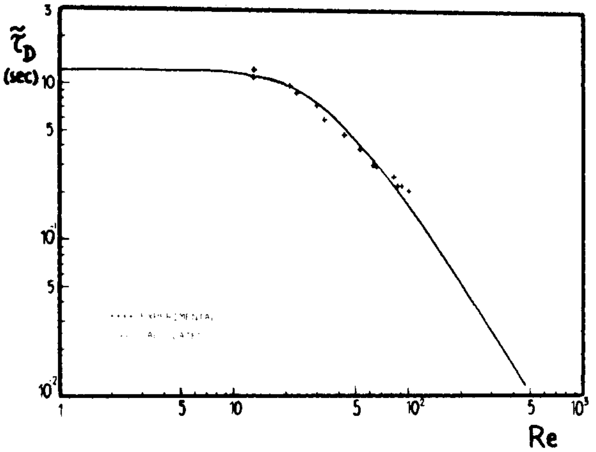

Figure 2. Comparison between experimental (apparent) diffusion time and calculated diffusion time, based on optimized values of permeability and true effective diffusivity (——).

pseudo-octahedric and (PO$_4$) tetrahedrical. Due to the spatial arrangements of these groups, a lamelar structure with high permeability is obtained. Details on the catalyst structure for the partial oxydation catalyst of butene can be found elsewhere (Bordes, 1980). The experimental results obtained by Ahn (1980) are summarized in Figure 1. Details on the experimental setup are given in the previous reference.

Diffusivity values obtained at Reynolds numbers (Re = $u_o d_p \rho/\mu$) higher than 100 are inaccurate since the input and output signals are very similar; at low Re (Re < 5), the axial dispersion has great influence on the overall measured variance. Then, intermediate ranges of Re are appropriate for measuring effective diffusivities. The results presented were derived on the basis of the simplified model which does not consider intraparticle-forced convection; that is the reason why we denote this apparent effective diffusivity by $\tilde{D}_{\text{eff}}$.

From the transfer function of the system values of $\tilde{\tau}_D$ and Pe were obtained by a two parameter optimization technique using identification of the transfer function for real values of s.

We have already explained the variation of $\tilde{D}_{\text{eff}}$ with Re.The true effective diffusivity, however, does not change with flowrate and should be obtained at low values of Reynolds number (if correct measures could be made). The apparent effective diffusivity, $\tilde{D}_{\text{eff}}$, increases with the flowrate due to the increase of the intraparticle convective flow, v_o with Re.

However, even if the trends are explained, one should be able to calculate v_o(Re) in another way, and then test our hypothesis. In fact, if there is a link between the pressure drops along the reactor (ΔP) and through the particle (Δp), we can get additional information. The pressure drop, ΔP through the fixed bed of length L, is given by the Ergun equation, modified by Scott et al. (1974) for the SPSR, i.e.,

$$\frac{\Delta P}{L} = \frac{150\mu(1-\epsilon)^2}{d_M^2 \epsilon^3} u_o + 1.75 \frac{\rho(1-\epsilon)}{d_M \epsilon^3} u_o^2 \tag{21}$$

where $d_M = d_p/(1 + \phi)$ and $\phi = (d_t/d_p)^2 L/N$ (N-number of particles in the tube) is a corrective factor for the SPSR.
Since the pressure drop, Δp in a particle of dimension l is

$$\frac{\Delta p}{l} = \frac{\mu}{B} v_o \tag{22}$$

where B is the particle permeability (cm^2) and $\Delta P/L = \Delta p/l$ we obtain from Eqs. 21 and 22:

$$v_o = a_1 B u_o + a_2 B u_o^2 \tag{23}$$

where $a_1 = 932.62$ and $a_2 = 43.62$.
Finally

$$\tilde{\tau}_D(\text{Re}) = F(\tau_D, B) = \frac{3}{F_1(B,\text{Re}) th\{\tau_D F_1(B,\text{Re})\}} - \frac{3}{\tau_D\{F_1(B,\text{Re}\}^2} \tag{24}$$

where $F_1(B,\text{Re}) = 4973.96\, B\text{Re} + 93.05\, B\text{Re}^2$; one easily notices that $\tau_C = 1/F_1(B,\text{Re})$.

Given the experimental set of values ($\tilde{\tau}_D$,Re), a two-parameter optimization by the Rosenbrock method was carried out leading

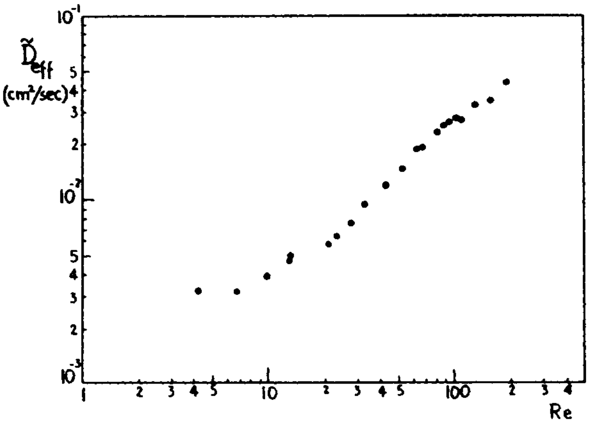

Figure 1. Experimental values of the apparent effective diffusivity as a function of the Reynolds number (hydrogen tracer in BM329 catalyst at 293 K).

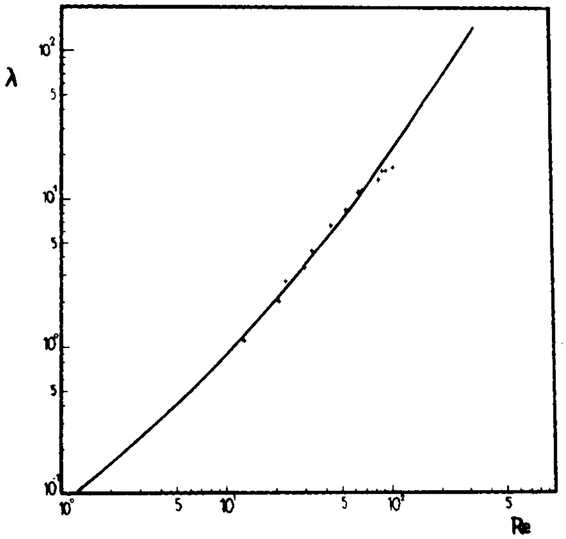

Figure 3. Intraparticle Peclet number as a function of the Reynolds number.

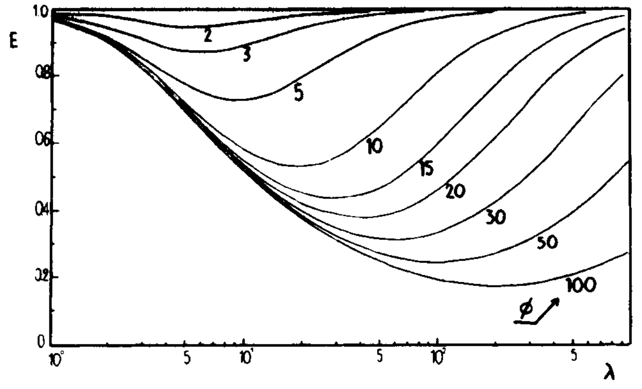

Figure 4. Effectiveness factors ratio, *E*, as a function of the intraparticle Peclet number, with the Thiele modulus as a parameter.

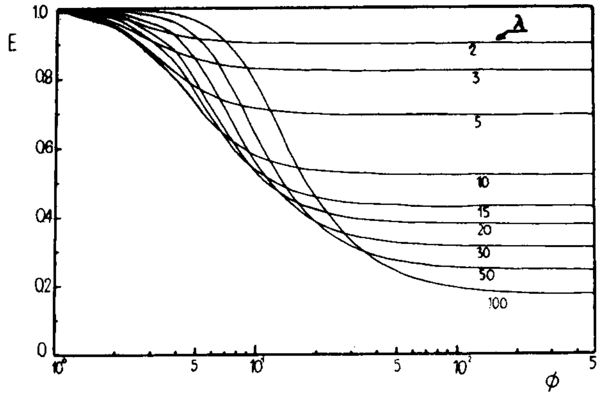

Figure 5. Effectiveness factors ratio, *E*, as a function of the Thiele modulus, with the intraparticle Peclet number as a parameter.

to $\tau_D = 1.216$ s and $B = 1.275 \times 10^{-5}$ cm^2. The true value of the effective diffusivity is then $D_{\text{eff}} = 4.625 \times 10^{-3}$ cm^2/s. Experimental points, $\tilde{\tau}_D$ and calculated points, $(\tilde{\tau}_D)_c$ by using Eq. 11 with the optimized values of τ_D and B are shown in Figure 2; the mean relative error is 8.5%. In Figure 3, the intraparticle Peclet number, λ, is plotted against the Reynolds number; a good agreement exits between predicted and experimental values.

Taking into account the value of the effective diffusivity, $D_{\text{eff}} = 4.625 \times 10^{-3}$ cm^2/s, one can calculate, by the model of Johnson and Stewart, a tortuosity factor $T = 79.6$. In this calculation, we used an intraparticle porosity $\beta = 0.537$ and a diffusivity of hydrogen in air, $D = 0.686$ cm^2/s; this last quantity was calculated by

$$D = \int_0^\infty \frac{f(r)dr}{\dfrac{1}{(D_K)_{H_2}} + \dfrac{1}{D_{H_2-\text{air}}}}$$

given the pore size distribution, $f(r)$, the Knudsen diffusivity, D_K, and the molecular diffusivity, $D_{H_2-\text{air}}$.

This high value of the tortuosity factor is due to the lamelar structure of the catalyst used. The value of the permeability is also very high ($\simeq 10^{-5}$ cm^2); however, as pointed out by Scheidegger (1974), values of B can vary in a large range ($10^{-5} - 10^{-6}$ for cork, $10^{-6} - 10^{-7}$ for sand, etc.); the spongy structure of the catalyst may justify such a value.

IMPLICATION OF INTRAPARTICLE-FORCED CONVECTION IN REACTOR DESIGN.

Let us now try to analyze the influence of neglecting intraparticle convection flow in reactor design.

Wheeler (1951) considered qualitatively the effect of the intraparticle convection term; it seems that this idea was not fully developed until very recently. Nir and Pismen (1977) and Nir (1977) discussed in two excellent papers the importance of intraparticle convection in catalysts for single and complex reactions, respectively. However,the comparison was made in terms of the ratio of the effectiveness factors calculated from the complete model and in the absence of convection.

It seems that for practical purposes one should compare the catalyst effectiveness factor taking into account the convection term with the apparent catalyst effectiveness factor calculated with the apparent effective diffusivity, $\tilde{D}_{\text{eff}}$ measured at a given flowrate. If, by chance, this ratio is equal to one, there is obviously no trouble with design, whatever the physical basis of the phenomenon.

The effectiveness factor for isothermal slab catalyst where a first-order irreversible reaction is going on and intraparticle convection and diffusion are considered is (Nir and Pismen, 1977)

$$\eta_{D-C} = \frac{1/\alpha_1 - 1/\alpha_2}{\coth\alpha_1 - \coth\alpha_2} \tag{25}$$

where $\alpha_1, \alpha_2 = \lambda/2 \pm \sqrt{\lambda^2/4 + \phi^2}$ and ϕ is the Thiele modulus based on the true effective diffusivity, D_{eff}.

The effectiveness factor based on a measured $\tilde{\tau}_D$ (and then $\tilde{D}_{\text{eff}}$), when the convective term is not taken into account in the model, is

$$\tilde{\phi} = \phi\sqrt{f(\lambda)} \tag{26}$$

since $\tilde{D}_{\text{eff}} = D_{\text{eff}}/f(\lambda)$. The corresponding effectiveness factor is then

$$\tilde{\eta} = \frac{th\tilde{\phi}}{\tilde{\phi}} = \frac{th(\phi\sqrt{f(\lambda)})}{\phi\sqrt{f(\lambda)}} \tag{27}$$

The ratio $E = \eta_{D-C}/\tilde{\eta}$ gives a measure of the error made when neglecting the influence of intraparticle convective flow and using an apparent effective diffusivity, $\tilde{D}_{\text{eff}}$ in Thiele modulus calculations.

Figures 4 and 5 show the E factor as a function of λ and ϕ respectively, using either ϕ or λ as parameters. The limiting situations are easily derived: for $\lambda = 0$, $E = 1$; as $\lambda \to \infty$, $E \to 1$ also for any ϕ. Curves of E vs. λ at constant ϕ show a minimum; similarly, plots of E vs. ϕ at constant λ show a plateau at high values of ϕ. This plateau is given by

$$E = \frac{\sqrt{f(\lambda)}}{th(\phi\sqrt{f(\lambda)})}\sqrt{1 + \frac{\lambda^2}{4\phi^2}} \tag{28}$$

and for high ϕ and λ, $E = \sqrt{3/\lambda}$. For certain values of ϕ and λ, one can get E values of 0.5, and so making errors of 100% in reactor design, Iso-E plots can be constructed in a ϕ-λ plan (Rodrigues, 1980b).

IN CONCLUSION

"Discrepancies" in current data of effective diffusivities as function of flowrate can be explained in terms of the influence of intraparticle-forced convection. This can readily occur in large pore catalysts, specially in liquid phase. Evaluation of errors in reactor design can be made and further work will extend this methodology to nonisothermal catalysts and complex reactions.

A systematic set of diffusivity measurements at different flowrates is also needed for bidisperse catalysts in order to fully understand the phenomenon. Coupling with permeability measurements would be of interest. Finally, checking the proposed explanation can be made in the presence of chemical reaction.

ACKNOWLEDGMENTS

A. E. Rodrigues is grateful to French Government and NATO Scientific Affairs Division for financial support and for INIC and University of Porto for the leave of absence. Rhone-Poulenc Industries is gratefully acknowledged for providing us with the catalyst used in the experiments. J. Villermaux (LSGC-CNRS, Nancy)

is greatly appreciated for his suggestion for the interpretation developed in the paper.

NOTATION

a = specific area of the particle, cm^{-1}
B = permeability of the particle, cm^2
Bi_m = Biot number, dimensionless
c = fluid-phase concentration, g/cm^3
c_o = inlet fluid-phase concentration, g/cm^3
c' = intraparticle fluid concentration, g/cm^3
d_p = particle diameter, cm
d_t = tube diameter, cm
$\bar{d}$ = mean pore diameter, cm
D_{eff} = true effective diffusivity, cm^2/s
$\tilde{D}_{eff}$ = apparent effective diffusivity, cm^2/s
D_{ax} = axial dispersion coefficient, cm^2/s
$G(s)$ = transfer function
l = half thickness of the catalyst particle, cm
L = reactor length, cm
N = number of particles in the reactor
Pe = Peclet number, dimensionless
$\Delta P, \Delta p$ = pressure drops in the reactor and in the particle, respectively, g/cm^2
Q = flowrate, cm^3/s
Re = Reynolds number, dimensionless
s = Laplace variable, s^{-1}
t = time, s
u_o = superficial velocity, cm/s
v_o = intraparticle convective velocity, cm/s
v_f, v_s = fluid and solid volumes in a perfectly mixed reactor, respectively, cm^2
x = particle space coordinate, cm
z = axial coordinate in the fixed-bed reactor, *cx*
z^* = reduced axial coordinate, dimensionless

Greek Letters

β = intraparticle porosity, dimensionless
ϵ = extraparticle porosity, dimensionless
γ = total porosity, dimensionless
λ = intraparticle Peclet number, dimensionless
ϕ = Thiele modulus based in the true effective diffusivity, dimensionless
$\tilde{\phi}$ = Thiele modulus based in the apparent effective diffusivity
$\eta_{D\text{-}C}$ = effectiveness factor based on the true diffusivity and intraparticle convection
$\tilde{\eta}$ = effectiveness factor based on the apparent effective diffusivity
ρ = fluid density, g/cm^3; reduced particle space coordinate, dimensionless
μ = fluid viscosity, cpoise
τ = space time, s
τ_C = intraparticle convection time, s
τ_D = intraparticle diffusion time, s
τ_f = external diffusion time, s
$\tilde{\tau}_D$ = apparent internal diffusion time, s

LITERATURE CITED

Ahn, B. J., "Étude des Caracteristiques Diffusionelles de Transfert de Matiére dans un Reacteur Catalytique à Lit Fixe d'Oxydation Menagée," Docteur-Ingenieur Dissertation, Univ. Techologie de Compiègne (1980).

Berty, J. M., "Reactor for Vapor Phase Catalytic Studies," *Chem. Eng. Prog.*, **70**(5), 78 (1974).

Boersma-Klein, W., and J. A. Moulijn, "The Evaluation in Time Domain of Mass Transfer Parameters from Chromatographic Peaks," *Chem. Eng. Sci.*, **34**, 959 (1979).

Bordes, E., "Properties Structurales de Phase Catalytiques à l'État Stationnaire: Application aux Systèmes (V-P-O),(V-M-O),(UMO) Selectifs dans l'Oxydation du Butène an Aydride Maleique," Docteu-ès-Sciences Dissortation, Unit. Technologie de de Compienge (1980).

Cerro, R., and J. M. Smith, "Chromatography of Nonadsorbable Gases," *AIChE J.*, **16**(6), 1034 (1970).

Choudary, V., "Gas Chromatographic Measurements of Transport Properties," *J. Chromatography*, **98**, 491 (1974).

Dogu, G., and J. M. Smith, "Rate Parameters from Dynamic Experiments with Single Catalyst Pellet," *Chem. Eng. Sci.*, **31**, 123 (1976).

Furusawa, T., M. Suzuki, and J. M. Smith, "Rate Parameters in Heterogeneous Catalysis by Pulse Techniques," *Cat. Rev. Sci. Eng.*, **13**(1), 43 (1976).

Kawazoe, K., and Y. Takeuchi, "Mass Transfer in Adsorption on Bidisperse Porous Materials," *J. Chem. Eng. Japan*, **7**(6), 431 (1974).

Nir, A., "Simultaneous Intraparticle Forced Convection, Diffusion and Reaction in a Porous Catalyst II-Selectivity of Sequential Reactions," *Chem. Eng. Sci.*, **32**, 925 (1977).

Nir, A., and L. M. Pismen, "Simultaneous Intraparticle Forced Convection, Diffussion and Reaction in a Porous Catalyst," *Chem. Eng. Sci.*, **32**, 35 (1977).

Rhone-Poulenc Industries, "Technical Bulletin on Catalyst," BM329 (1980).

Rodrigues, A. E., "Intraparticle Forced Convection Effect in Porous Catalyts," *Internal Report*, Univ. Tech. Compiègne (1980).

Rodrigues, A. E., "The Scientific Basis for the Design of Catalytic Reactors," *Multiphase Chemical Reactors*, to be published by Sijthoff & Noordhoff.

Scheidegger, A., *The Physics of Flow Through Porous Media*, Univ. Toronto Press (1974).

Scott, D., W. Lee, and J. Papa, "The Measurement of Transport Coefficients in Gas-Solid Heterogenous Reactions," *Chem. Eng. Sci.*, **29**, 2155 (1974).

Smiljanic, D., "Diffusivity and Structure of Porous Pellets," *J. Catalysis*, **46**, 214 (1977).

Wheeler, A., "Reaction Rate and Selectivity in Catalyst Pores," *Adv. Catalysis*, 3, 250 (1951).

Wicke, E., and R. Kallenbach, "Die Oberflachendiffusion von Kohlendioxyd in Aktiven Kohlen," *Kolloid-Z*, **97**(2), 135 (1941).

Youngquist, G. R., "Diffusion and Flow of Gases in Porous Solids," *Ind. Eng. Chem.*, **62**(8), 52 (1970).

Manuscript received December 23, 1980, revision received September 2, and accepted September 16, 1981.